

# Titania-supported cobalt and nickel bimetallic catalysts for carbon dioxide reforming of methane

Kazuhiro Takanabe<sup>a</sup>, Katsutoshi Nagaoka<sup>b,c</sup>, Kentaro Nariai<sup>a</sup>, Ken-ichi Aika<sup>a,b,\*</sup>

<sup>a</sup> Department of Environmental Chemistry and Engineering, Interdisciplinary Graduate School of Science and Engineering, Tokyo Institute of Technology, 4259 Nagatsuta, Midori-ku, Yokohama 226-8502, Japan

<sup>b</sup> CREST, JST (Japan Science and Technology Corporation), Japan

<sup>c</sup> Department of Applied Chemistry, Faculty of Engineering, Oita University, Dannoharu 700, Oita 870-1192, Japan

Received 29 November 2004; revised 10 March 2005; accepted 13 March 2005

Available online 25 April 2005

## Abstract

Titania-supported cobalt and nickel bimetallic catalysts were investigated for CO<sub>2</sub> reforming of methane to synthesis gas at 1023 K under ambient pressure. Bimetallic Co–Ni/TiO<sub>2</sub> catalysts with an appropriate Co/Ni ratio showed highly stable activities without carbon deposition. Whereas the monometallic Co/TiO<sub>2</sub> catalyst deactivated rapidly because of the oxidation of metal, 10 mol% substitution of nickel for cobalt suppressed the oxidation of metal, providing a high catalytic stability. However, the catalysts with excess nickel content (>80 mol%) underwent carbon formation. X-ray diffraction (XRD) and X-ray photoelectron spectroscopy (XPS) analyses revealed that a homogeneous alloy of cobalt and nickel was formed from bulk to the surface by the H<sub>2</sub> reduction, and the alloy was stable during reforming. The advantages of the bimetallic catalysts are high resistance to undesirable metal oxidation and coking, through the control of reactions between CH<sub>4</sub> and CO<sub>2</sub>.

© 2005 Elsevier Inc. All rights reserved.

**Keywords:** Cobalt; Nickel; Bimetal; Alloy; Titania; Methane; CO<sub>2</sub> reforming; Strong resistance to coking

## 1. Introduction

Carbon dioxide reforming of methane to synthesis gas (CH<sub>4</sub> + CO<sub>2</sub> ⇌ 2CO + 2H<sub>2</sub>) has been of great interest for the technology of natural gas conversion, since the reaction can optimize the H<sub>2</sub>/CO ratio when combined with, for instance, steam reforming of methane. In general, carbon formation on catalysts is a serious issue for the reaction. Supported noble metals, such as Rh, Ru, Pd, Pt, and Ir, can provide operations with lower carbon deposition in the CH<sub>4</sub>/CO<sub>2</sub> reaction [1]. However, from a practical point of view, noble metals are unsuitable for industrial use, considering their high cost and restricted availability. Hence, supported Ni cat-

alysts are commonly applied because of their low cost [2]. The nickel catalysts are known to show high catalytic activity; however, nickel catalysts easily induce formation of graphitic carbon, causing catalyst deactivation and plugging of a reactor tube [1,2].

There have been a number of discussions on how to avoid carbon formation [3,4]. A number of contributions have claimed that the nature of the supports strongly affects the catalytic behavior and carbon deposition for the CH<sub>4</sub>/CO<sub>2</sub> reaction [5–10]. Among oxides titania is reported to be an excellent support for suppressing carbon deposition [5–7, 10–16]. It is proposed that during H<sub>2</sub> reduction, the partially reduced TiO<sub>x</sub> species would migrate on the metal particle (so-called strong metal support interaction (SMSI) [17,18]), destroy large ensembles of the metal species, and create the highly active sites for the reforming at the boundary between metal and support, resulting in reduction of the amount of carbon deposits [7,11].

\* Corresponding author. Fax: +81 45 924 5441.

E-mail addresses: [takanabe@chemenv.titech.ac.jp](mailto:takanabe@chemenv.titech.ac.jp) (K. Takanabe), [nagaoka@cc.oita-u.ac.jp](mailto:nagaoka@cc.oita-u.ac.jp) (K. Nagaoka), [nariai@chemenv.titech.ac.jp](mailto:nariai@chemenv.titech.ac.jp) (K. Nariai), [kenaika@chemenv.titech.ac.jp](mailto:kenaika@chemenv.titech.ac.jp) (K. Aika).

Another idea for minimizing carbon deposits is preventing carbide formation on the metal particles, because carbide formation is suggested to be the essential intermediate for carbon formation [4]. It has been reported that doping Ni catalysts with other metal, such as tin [19], chromium [20,21], or manganese [22,23], has a significant effect on the suppression of carbide formation. Some detailed studies [24,25] have shown that additives like potassium, sulfur, and gold preferentially bind to the step sites working as the coking sites and, hence, suppress graphite formation, without significantly influencing the catalytic activity for the reforming.

It has also been reported that the addition of cobalt to nickel catalysts reduces coke formation during reactions, such as CO methanation [26], partial oxidation of methane to synthesis gas [27,28], and steam or CO<sub>2</sub> reforming of methane [29]. Bartholomew et al. suggested that suppression of coke formation by the addition of cobalt to nickel catalyst for CO methanation would be due to enhancement of the hydrogenation of atomic carbon and/or inhibition of the formation of carbide species in the metal crystal [26]. However, the beneficial effects and the nature/state of the bimetallic catalysts remain unclear and needed to be investigated.

Cobalt has attracted interest as an active metal for the CO<sub>2</sub> reforming of methane [13–16,30]. The authors have studied the CO<sub>2</sub> reforming of methane over 0.5 wt% Co/TiO<sub>2</sub> at 2.0 MPa, where carbon formation is highly favored, as predicted by thermodynamic equilibrium [13,14]. The Co/TiO<sub>2</sub> catalyst showed a high tolerance to carbon deposition but gradually deactivated because of the oxidation of the metallic cobalt. In fact, a partial substitution of nickel for cobalt (typically Co/Ni = 90/10) enhanced catalytic stability dramatically [15]. It is speculated that, by accelerating methane decomposition, the nickel provides reductive hydrogen to the cobalt via spillover phenomena [31,32], thus inhibiting oxidation of the cobalt. However, it is difficult in practice to clarify the state of the bimetallic catalysts because of the necessity for low metal loading (0.5 wt%) for high-pressure operations.

At atmospheric pressure, higher loading of the metal can also be applied for stable operations [13], and 10 wt% Co/TiO<sub>2</sub> was investigated thoroughly [16]. It is proposed that, during CH<sub>4</sub>/CO<sub>2</sub> reforming, the reactions between CH<sub>4</sub> and CO<sub>2</sub> should be balanced appropriately [16,30]. The coke species formed by decomposition of CH<sub>4</sub> on the metal has to be removed by the activated oxygen species derived from CO<sub>2</sub>. The cobalt catalysts tended to be deactivated by oxidation of the metal, implying that the oxygen species derived from CO<sub>2</sub> reacts more preferentially than the coke species derived from CH<sub>4</sub>.

This contribution pertains to the carbon dioxide reforming of methane over the bimetallic Co–Ni/TiO<sub>2</sub> catalysts (metal loading 10 wt% in total) at atmospheric pressure. The purpose of this work is to combine the nature of cobalt (stronger affinity for oxygen species) and with that of nickel (stronger affinity for carbon species) and to suppress both

metal oxidation and carbon formation. Catalysts with various Co/Ni ratios have been prepared and tested for CO<sub>2</sub> reforming of CH<sub>4</sub>. To clarify the beneficial effects of the bimetallic catalysts, the state and nature of the Co–Ni/TiO<sub>2</sub> catalysts have been extensively characterized.

## 2. Methods

### 2.1. Catalyst preparation

Co–Ni/TiO<sub>2</sub> catalysts were prepared by incipient wetness co-impregnation of an aqueous solution of Co(NO<sub>3</sub>)<sub>2</sub> · 6H<sub>2</sub>O and Ni(NO<sub>3</sub>)<sub>2</sub> · 6H<sub>2</sub>O (Wako Pure Chemical Industries Ltd.) with TiO<sub>2</sub> (Ishihara Sangyo; A-100, anatase phase), which is pre-calcined at 773 K for 15 h. The metal loading was set at 10 wt% for Co/TiO<sub>2</sub>, and cobalt was replaced with the same moles of nickel. The catalysts were dried at room temperature and then at 373 K overnight, followed by calcination at 673 K for 4 h in flowing air to remove ligands from the cobalt and nickel precursors. The powder-form catalysts were pressed into pellets, crushed, and sieved to obtain grains with diameters between 600 and 900 μm. Catalyst with the ratio Co/Ni = *m*:*n* are denoted CoNi(*m*:*n*)/TiO<sub>2</sub>.

### 2.2. Catalyst characterization

Temperature-programmed reduction (TPR) measurements were carried out over 0.1 g of the calcined catalysts from room temperature to 1223 K, at a rate of 10 K min<sup>-1</sup> in flowing H<sub>2</sub>/Ar gas (5:95 vol/vol mixture with a total flow of 30 ml min<sup>-1</sup>). The hydrogen consumption was monitored with a TCD.

The specific surface area of the catalysts after H<sub>2</sub> reduction was determined by the BET method. The amounts of chemisorbed CO were determined by a pulse method. Typically 0.1 g of catalyst was reduced in situ at 1123 K for 1 h in a H<sub>2</sub> flow and flushed with He (>99.999% purity) at each temperature for 15 min. Pulses (pulse volume 1.08 ml) of 1% CO in He gas were injected through the catalysts at room temperature until no further adsorption of CO was detected with a TCD.

XRD analysis was performed with a Rigaku Multiflex X-ray diffractometer with monochromatized Cu-K<sub>α</sub>. Metal crystallite sizes were calculated from line broadening with the Scherrer equation [33].

X-ray photoelectron spectroscopy (XPS) was performed with an ULVAC-PHI model 3057 ESCA system with a monochromatized Al-K<sub>α</sub> (1486.7 eV, 200 W) under a pressure of approximately 10<sup>-9</sup> Torr. After the reduction, the catalysts were flushed with helium gas and kept in a closed vial, then transferred into the spectrometer without exposure to the ambient air. The measurements were carried out under approximately 1.0 × 10<sup>-6</sup> Pa, and the C 1s peak at 284.8 eV was used as a reference. To compensate for lost electrons

during the measurements, a pass energy of 23.5 eV was used for all samples.

Deposited carbon was quantified by a temperature-programmed oxidation (TPO) method. After the reaction, the catalyst was heated to 1273 K at a rate of 10 K min<sup>-1</sup> in an O<sub>2</sub>/He mixture (5:95 vol/vol with a total flow of 50 ml min<sup>-1</sup>). CO<sub>x</sub> gases derived from deposited carbon were passed through a methanator and then monitored with a flame ionization detector (FID).

TPO in CO<sub>2</sub> measurement was carried out to investigate the oxidation behavior of the reduced catalysts. The increase in the catalyst weight during oxidation of the reduced catalyst in flowing CO<sub>2</sub> was monitored by differential thermogravimetry (TG), performed with SSC/5200, SII. The temperature was increased from room temperature to 1223 K, at a rate of 10 K min<sup>-1</sup>.

CH<sub>4</sub> pulse reaction was carried out to investigate the reactivity of the catalysts to CH<sub>4</sub>. After in situ reduction, high-purity CH<sub>4</sub> pulses (99.999%, pulse size 44.1 μmol) were injected at 1023 K in Ar carrier (flow rate 30 ml min<sup>-1</sup>) over 100 mg of the catalyst. The reactant and product gases were separated by an active carbon column and detected with a TCD. In addition to the expected product (H<sub>2</sub> and C remaining on the catalyst surface), CO was observed in a small quantity, which was probably derived from the reaction between CH<sub>4</sub> and impurities in the Ar carrier. However, the amount produced was small (<2 μmol), and therefore the total amount of converted CH<sub>4</sub> was used to determine the catalytic activity.

### 2.3. CH<sub>4</sub>/CO<sub>2</sub> reaction

All catalysts were tested at atmospheric pressure. Typically 0.5 g of the catalyst was loaded into a fixed-bed tubular inconel reactor (i.d. 6 mm). The axial temperature profile was measured for the furnace without the catalyst bed. Subsequently, the catalyst was placed in the isothermal zone of the furnace. The catalysts were reduced in situ in a H<sub>2</sub> flow at 1123 K for 1 h. The reaction temperature was set at 1023 K. CH<sub>4</sub>/CO<sub>2</sub> gases were introduced into the catalyst bed at a total flow rate of 50 N ml min<sup>-1</sup> (space velocity (SV) 6000 ml g<sub>cat</sub><sup>-1</sup> h<sup>-1</sup>). During the reaction, temperature at the inlet of the catalyst bed was measured (where the reaction was expected to occur to the largest extent). Throughout the series of experiments, the temperature decrease in the catalyst bed due to the reaction was very small (1–2 K). Further details of the procedure and apparatus have been described elsewhere [16].

## 3. Results

### 3.1. The state of the reduced Co–Ni/TiO<sub>2</sub> catalysts

For the CoNi(50:50)/TiO<sub>2</sub> calcined at 673 K (before reduction) Co<sub>3</sub>O<sub>4</sub> and NiO were observed in separate phases,

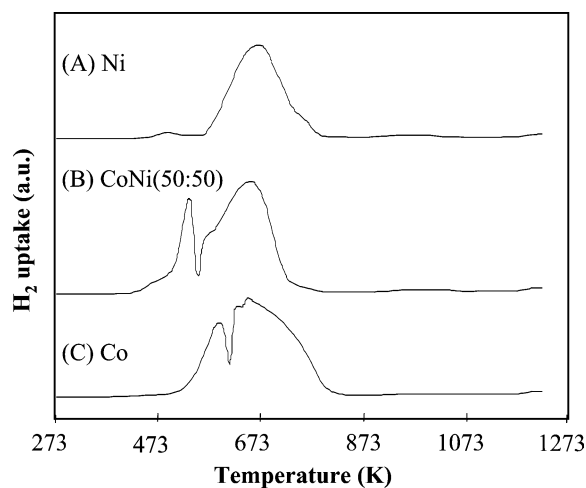


Fig. 1. TPR profiles for (A) Ni/TiO<sub>2</sub>, (B) CoNi(50:50)/TiO<sub>2</sub>, and (C) Co/TiO<sub>2</sub>.

which was confirmed by XRD analysis (not shown). Fig. 1 shows TPR profiles for the Ni/TiO<sub>2</sub>, CoNi(50:50)/TiO<sub>2</sub>, and Co/TiO<sub>2</sub> catalysts calcined at 673 K. For Ni/TiO<sub>2</sub> one peak was observed, from around 600 K to around 800 K with the maximum at 690 K, corresponding to the reduction of NiO to Ni<sup>0</sup>. For Co/TiO<sub>2</sub> two continuous peaks were observed; one was observed at 490–650 K and the other ended below 850 K. These results indicate that the reduction of Co<sub>3</sub>O<sub>4</sub> to CoO occurred first, followed by reaction to metallic Co [34]. For the bimetallic catalyst the peaks were observed to start at a lower temperature of 460 K and end at 700 K. Two or more overlapped peaks were observed, which can be assigned to simultaneous reduction of Co<sub>3</sub>O<sub>4</sub> and NiO. Note that all nickel and cobalt oxides were reduced completely at the reduction temperature of 1123 K in this study.

In Table 1, the amounts of CO chemisorbed on reduced Co–Ni/TiO<sub>2</sub> with different Co/Ni ratios are shown. The amounts of chemisorbed CO increased with increasing Ni content (Co/TiO<sub>2</sub>, 1.08 μmol g<sup>-1</sup>; Ni/TiO<sub>2</sub>, 2.20 μmol g<sup>-1</sup>). It should be noted that the values were fairly small for all catalysts (0.06–0.13% dispersion, assuming CO/metal = 1 stoichiometry). This may be partly ascribed to the strong metal support interaction phenomena of TiO<sub>2</sub> [17,18] taking place during high-temperature reduction (1123 K), which is discussed in the earlier report [16]. Alternatively, the specific surface area of the catalysts did not vary among the catalysts (for Co/TiO<sub>2</sub> it was 5 m<sup>2</sup> g<sub>cat</sub><sup>-1</sup>, and for Ni/TiO<sub>2</sub>, 3 m<sup>2</sup> g<sub>cat</sub><sup>-1</sup>), strongly depending on the structure of support TiO<sub>2</sub> after the reduction at 1123 K (rutile phase).

Fig. 2(I) shows the XRD patterns for Co/TiO<sub>2</sub>, CoNi(50:50)/TiO<sub>2</sub>, and Ni/TiO<sub>2</sub> after the reduction at 1123 K. After the reduction, the metallic phase of cobalt and nickel was observed. A phase transfer of TiO<sub>2</sub> from anatase to rutile was also observed. There is hardly any difference in TiO<sub>2</sub> structure among these three catalysts after reduction. To investigate the metallic cobalt and nickel more intensely, narrow scanning on the metallic phase was carried out. Fig. 3(I)

Table 1  
CO chemisorption capacity, metal crystallite size, turn over frequency and the amount of deposited carbon for Co–Ni/TiO<sub>2</sub> with different Co/Ni ratio

Co:Ni	The amount of CO chemisorbed ( $\mu\text{mol g}_{\text{cat}}^{-1}$ )	Metal crystallite size <sup>a</sup> (nm)		Turn over frequency for CH <sub>4</sub> at 1 h ( $\text{s}^{-1}$ )	Carbon amount (wt%)
		Before reaction <sup>a</sup>	After reaction		
0:100	2.20	34	36	4.7	0.93
10:90	1.91	37	33	4.9	1.05
20:80	1.79	37	36	4.1	0.25
50:50	1.83	33	34	4.0	0.07
80:20	1.44	37	38	4.2	n.d. <sup>c</sup>
90:10	1.48	34	37	4.2	n.d. <sup>c</sup>
100:0	1.08	33	41 <sup>b</sup>	1.0	n.d. <sup>c</sup>

<sup>a</sup> Calculated from line broadening using the Scherrer's equation [33].

<sup>b</sup> CoTiO<sub>3</sub> phase was formed after the CH<sub>4</sub>/CO<sub>2</sub> reaction.

<sup>c</sup> n.d. (not detected) represents below 0.01 wt%.

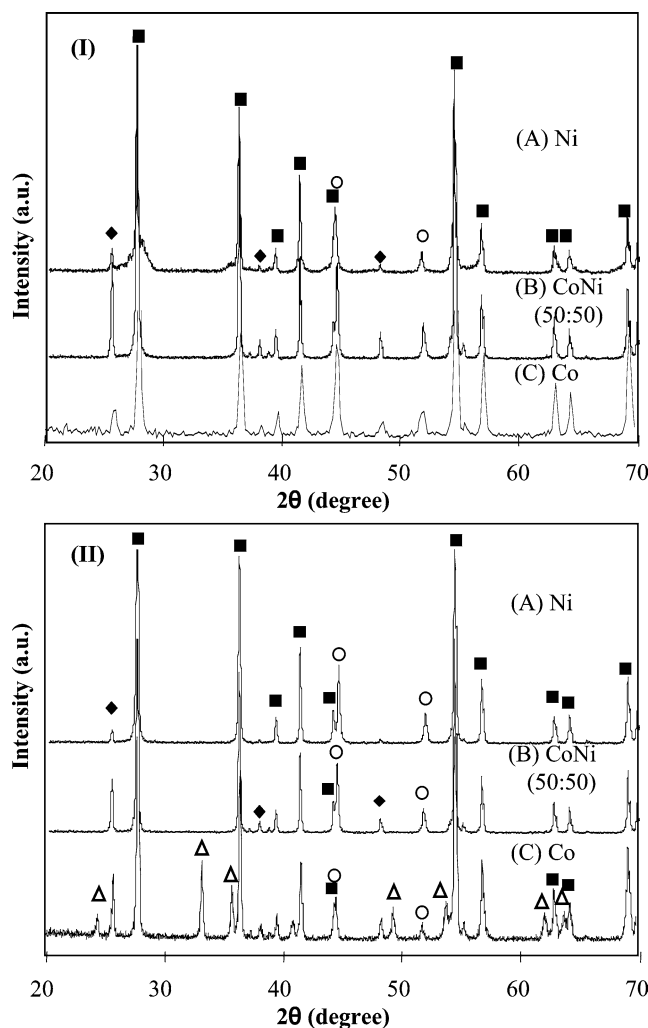


Fig. 2. XRD patterns for (A) Ni/TiO<sub>2</sub>, (B) CoNi(50:50)/TiO<sub>2</sub>, and (C) Co/TiO<sub>2</sub> (I) before and (II) after the reaction. (○) Co<sup>0</sup> or Ni<sup>0</sup>; (◆) TiO<sub>2</sub>-anatase; (■) TiO<sub>2</sub>-rutile; (Δ) CoTiO<sub>3</sub>.

shows XRD diffraction lines for the reduced catalysts. The line assigned to TiO<sub>2</sub> rutile (44.05°) was used as the internal standard to obtain reliable shifts of the peaks of the metals. The XRD pattern in a physically mixed sample of the reduced catalysts (shown at the top of Fig. 3(I)) showed two

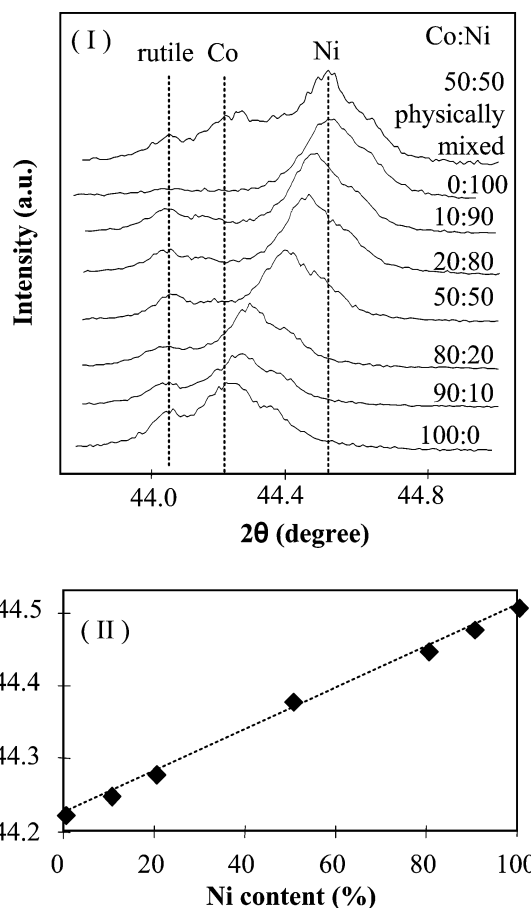


Fig. 3. (I) XRD patterns for the reduced Co–Ni/TiO<sub>2</sub> with different Co/Ni ratio and (II) Co/Ni ratio vs. peak maximum for the facet (111) of Co and/or Ni.

separate peaks for the metals assigned to cobalt (44.22°) and nickel (44.51°). In contrast, only one peak for the metals was observed for all of the Co–Ni/TiO<sub>2</sub> catalysts. Fig. 3(II) shows the Ni content (in mol%) versus the 2θ value of the peak. It can clearly be seen from Fig. 3(II) that the maxima of the metallic peak were shifted in proportion to the Co/Ni ratio. This reveals the formation of a homogeneous alloy of Co and Ni during the reduction for all of the bimetallic catalysts. Based on the assumption that all of the cobalt and

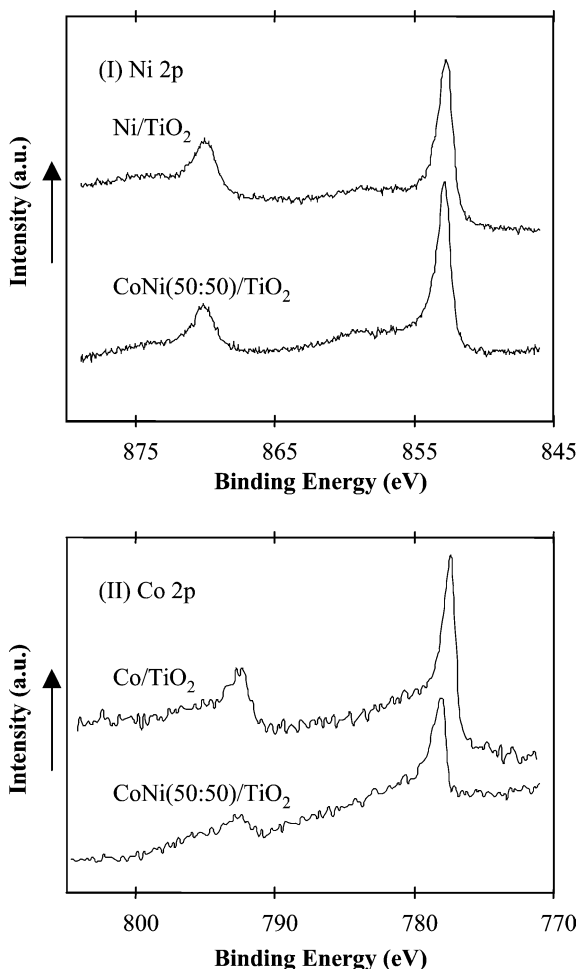


Fig. 4. XPS spectra for reduced Ni/TiO<sub>2</sub>, CoNi(50:50)/TiO<sub>2</sub>, and Co/TiO<sub>2</sub>. (I) Ni 2*p*. (II) Co 2*p*.

nickel formed alloy by the reduction, the crystallite sizes of the metal were estimated from XRD line broadening; these are listed in Table 1. The crystallite sizes were comparable for all of the reduced catalysts (33–37 nm).

The XRD results indicated the formation of alloy of Co and Ni in the bulk of the catalysts. XPS analysis was used to obtain information on the surface state of the alloy. Fig. 4(I) shows XP spectra for Ni 2*p*. For the Ni/TiO<sub>2</sub> catalyst the spectrum exhibited a peak at 852.7 eV, and for CoNi(50:50)/TiO<sub>2</sub> the peak was observed at 852.8 eV and assigned to metallic nickel. Fig. 4(II) for Co 2*p* shows the peak at 777.5 eV for Co/TiO<sub>2</sub> and 777.4 eV for CoNi(50:50)/TiO<sub>2</sub>, assigned to metallic cobalt. It is confirmed that all of the metal oxides were reduced on all of the catalysts. In addition, the Co/Ni ratio for CoNi(50:50)/TiO<sub>2</sub> was 45:55, indicating that the nearly stoichiometric surface composition of cobalt and nickel was also obtained as the bulk composition of the metals for CoNi(50:50)/TiO<sub>2</sub>. No evidence of electronic effects due to alloying of cobalt and nickel, such as transfer of *d*-electrons between metals [35], was observed for CoNi(50:50)/TiO<sub>2</sub>.

### 3.2. Catalytic performance over Co–Ni/TiO<sub>2</sub> and the state of the used catalysts

Fig. 5 shows CH<sub>4</sub> conversion versus time on stream over Co–Ni/TiO<sub>2</sub> with different Co/Ni ratios. The turnover frequency (TOF) was calculated from the CO chemisorption capacity, assuming that the surface state remained unchanged during the reaction; this is given in Table 1. It can be seen from Fig. 5 that, whereas the Co/TiO<sub>2</sub> catalyst lost its activity during the initial stage of the reaction, CoNi(90:10)/TiO<sub>2</sub> showed much higher and more stable activity (CH<sub>4</sub> conversion 34%). The catalytic activity increased gradually with increasing Ni content (CH<sub>4</sub> conversion 50.6% for Ni/TiO<sub>2</sub>). Remarkably, the deactivation was not observed for 24 h for all of the Co–Ni/TiO<sub>2</sub> and Ni/TiO<sub>2</sub> catalysts. In terms of TOF, CoNi(90:10)/TiO<sub>2</sub> improved dramatically. Among the catalysts with a Co/Ni ratio of 90:10 to 20:80, the values were very similar (4.0–4.2 s<sup>-1</sup>). It can be inferred that the cobalt and nickel catalyze the reaction

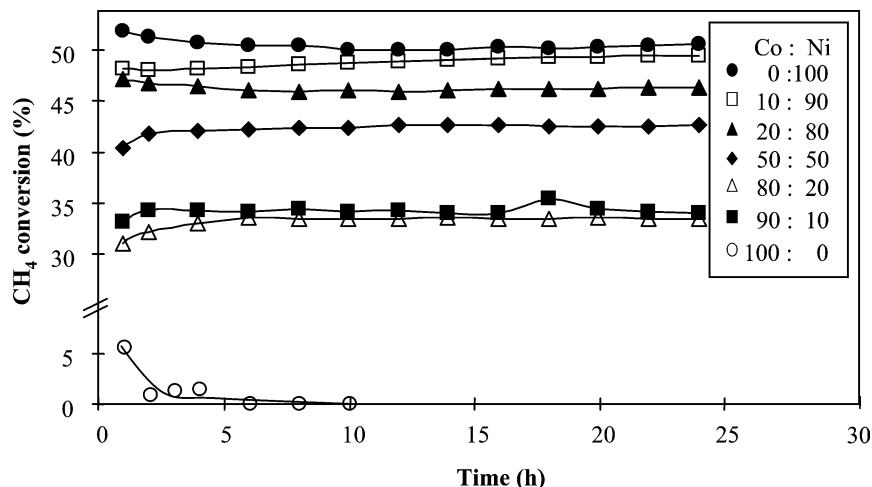


Fig. 5. Time on stream vs. CH<sub>4</sub> conversion for Co–Ni/TiO<sub>2</sub> with different Co/Ni ratio. (Reaction conditions: CH<sub>4</sub>/CO<sub>2</sub> = 1; 1023 K; 0.1 MPa; SV = 6000 ml g<sub>cat</sub><sup>-1</sup> h<sup>-1</sup>.)



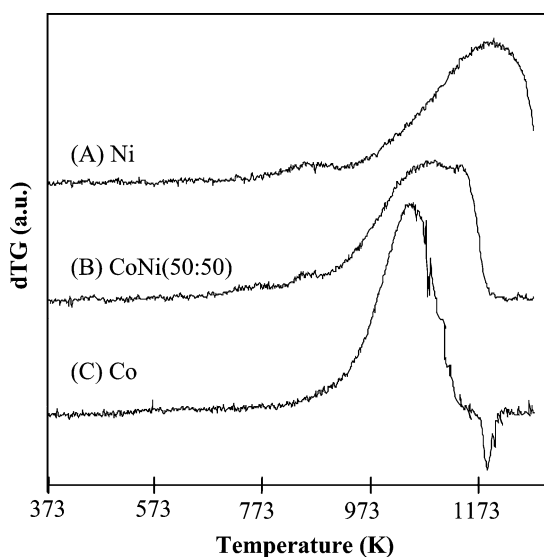


Fig. 6. dTG profiles of TPO in  $\text{CO}_2$  for (A)  $\text{Ni}/\text{TiO}_2$ , (B)  $\text{CoNi}(50:50)/\text{TiO}_2$ , (C)  $\text{Co}/\text{TiO}_2$ .

equivalently over these catalysts. The  $\text{CoNi}(10:90)/\text{TiO}_2$  and  $\text{Ni}/\text{TiO}_2$  catalysts showed slightly higher TOFs (4.9 and  $4.7 \text{ s}^{-1}$ , respectively). Thermodynamic equilibrium for  $\text{CH}_4$  conversion at 1023 K is 83.4%, which is far above the observed values. To determine whether mass transfer limitations existed, the following measurements were also carried out. First, changing the catalyst weight and reactant space velocity simultaneously, to keep the contact time the same, did not affect conversion values. Subsequently, the same experiment conducted with a smaller catalyst grain size did not show a significant difference in conversions. It was therefore concluded that external and internal mass transfer limitations can be neglected, and the measurements were carried out under the kinetic domain.

Table 1 also lists the amounts of carbon deposited on the catalysts after the reaction for 24 h. The  $\text{Co}/\text{TiO}_2$  catalyst, which showed fairly low activity, did not experience any carbon formation. The amounts of carbon increased slightly with increasing Ni content in the catalyst. In particular, more carbon was formed over the catalysts with high nickel content,  $\text{CoNi}(90:10)/\text{TiO}_2$  (1.05 wt%) and  $\text{Ni}/\text{TiO}_2$  (0.93 wt%). It should be noted that the yield of carbon was still negligible compared with the yield of CO; for example, for  $\text{Ni}/\text{TiO}_2$  the yield of carbon was approximately 0.01%, whereas the yield of CO was 56.6%.

The XRD patterns for the catalysts after 24 h of catalytic tests are shown in Fig. 2(II). It can be seen for all of the catalysts that the  $\text{TiO}_2$  rutile phase remained nearly the same. For  $\text{Co}/\text{TiO}_2$ , the  $\text{CoTiO}_3$  phase was observed and the intensity of the metallic cobalt phase decreased during the reaction, indicating that the oxidation of cobalt had taken place [16]. The metallic phases in XRD patterns after the reaction for all of the bimetallic catalysts and nickel catalyst were still observed, and the  $2\theta$  values of peak maxima remained unchanged before and after the reaction (not shown),

Table 2  
 $\text{CH}_4$  decomposition<sup>a</sup> over  $\text{Co}/\text{TiO}_2$ ,  $\text{CoNi}(50:50)/\text{TiO}_2$  and  $\text{Ni}/\text{TiO}_2$

Catalyst (metal)	The amount of $\text{CH}_4$ converted ( $\mu\text{mol}$ )	$\text{TON}_{\text{CH}_4}$ <sup>b</sup>
Ni	19.37	88.1
$\text{CoNi}(50:50)$	12.87	70.3
Co	4.68	43.3

<sup>a</sup> 44.1  $\mu\text{mol}$  of  $\text{CH}_4$  was pulsed.

<sup>b</sup> Turn over number (TON) was calculated from the mole of the reacted  $\text{CH}_4$  divided by the mole of the chemisorbed CO.

suggesting that the state of the alloy was sustained during the reaction. The crystallite sizes remained constant during the reaction regardless of the Co/Ni ratio (see Table 1), suggesting that the degree of sintering was not significant for any of the catalysts.

Oxidation of the metal can be a cause of deactivation, as observed in the case of  $\text{Co}/\text{TiO}_2$  [16]. To investigate the oxidation behavior of the reduced catalysts, TPO was carried out with  $\text{CO}_2$ ; the profiles are shown in Fig. 6.  $\text{CoNi}(50:50)/\text{TiO}_2$  showed a peak at around 1060 K, and the peak ended below 1180 K. Compared with  $\text{Co}/\text{TiO}_2$  catalyst (the peak at 1030 K), the temperature of the oxidation peak was 30 K higher, indicating higher tolerance to oxidation of metal. For  $\text{Ni}/\text{TiO}_2$ , the oxidation temperature of nickel is much higher than that of  $\text{Co}/\text{TiO}_2$  and  $\text{CoNi}(50:50)/\text{TiO}_2$  (the peak at 1180 K). After the measurements, it was confirmed by XRD analysis that titanate phases were formed in all of the catalysts, that is,  $\text{CoTiO}_3$  and  $\text{NiTiO}_3$  (not shown).

Activation of  $\text{CH}_4$  is considered to be the initial and a very important step for reforming [1]. Hence,  $\text{CH}_4$  pulse reaction (in the absence of  $\text{CO}_2$ ) was carried out over  $\text{Ni}/\text{TiO}_2$ ,  $\text{CoNi}(50:50)/\text{TiO}_2$ , and  $\text{Co}/\text{TiO}_2$ ; the results are compiled in Table 2. It can be seen that the activity for  $\text{CH}_4$  decomposition (both net conversion and TON) is in the order  $\text{Ni}/\text{TiO}_2 > \text{CoNi}(50:50)/\text{TiO}_2 > \text{Co}/\text{TiO}_2$ , indicating that  $\text{CH}_4$  decomposition is more facile over the catalysts with higher Ni content.

## 4. Discussion

### 4.1. The state and catalytic behavior of the bimetallic Co–Ni/ $\text{TiO}_2$ catalysts

First of all, the state of the metal in the bimetallic catalysts will be discussed. The XRD analysis showed only one peak for the metallic phase for the Co–Ni/ $\text{TiO}_2$  catalysts (Fig. 3(I)). As seen in Fig. 3(II), the shift of the metallic peak from cobalt to nickel was observed in proportion to the Co/Ni ratio, indicating the formation of alloy in the bulk of the catalysts. The surface Co/Ni composition for  $\text{CoNi}(50:50)/\text{TiO}_2$  had an almost stoichiometric value (Co/Ni = 45:55), which was confirmed by XPS analysis. The formation of uniform alloy from bulk to surface can be achieved during the reduction starting from the separate NiO

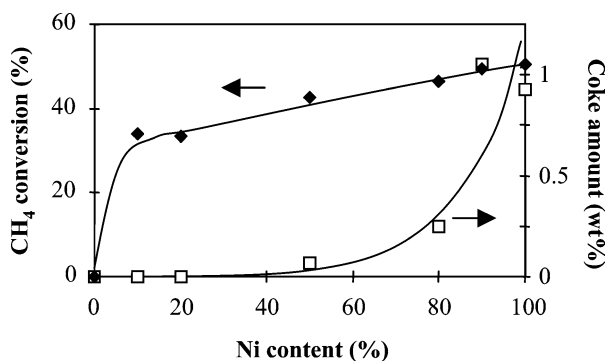


Fig. 7. Co/Ni ratio vs. CH<sub>4</sub> conversion and coke amount for Co–Ni/TiO<sub>2</sub>. (Reaction conditions: CH<sub>4</sub>/CO<sub>2</sub> = 1; 1023 K; 0.1 MPa; SV = 6000 mlg<sub>cat</sub><sup>-1</sup> h<sup>-1</sup>.)

and Co<sub>3</sub>O<sub>4</sub> phases. It was also confirmed that the state of the alloy remained unchanged during the CH<sub>4</sub>/CO<sub>2</sub> reforming.

The Co–Ni alloy catalysts showed highly stable activities for CH<sub>4</sub>/CO<sub>2</sub> reforming. It can be seen from Fig. 5 that the monometallic Co/TiO<sub>2</sub> catalyst deactivated rapidly. Since no carbon formation was observed (Table 1) and the XRD analysis indicated the formation of the titanate phase after the reaction (Fig. 2(II)(C)), the low activity and deactivation of Co/TiO<sub>2</sub> are attributed to the oxidation of metal, which was discussed thoroughly in the earlier report [16]. The small amount of substitution (10 mol%) of nickel for cobalt improved the catalytic activity and stability dramatically, suppressing the oxidation of metallic cobalt. The CH<sub>4</sub> conversion increased gradually with increasing Ni content (see Fig. 5). The carbon amount increased drastically with the introduction of higher Ni content (>80%). Although the carbon formed during the reaction did not cause the deactivation in this study, the accumulation of deposited carbon on the catalyst may cause an undesirable pressure drop or blockage of the reactor [1,2]. The correlation between conversions and coke amounts as a function of Ni content is shown in Fig. 7. It can be seen that an inhibition of oxidation observed over monometallic Co/TiO<sub>2</sub> is achieved by the addition of small amounts of Ni in the catalyst, and the suppression of carbon formation that occurred over the catalyst with high Ni content is achieved by the addition of appropriate amounts of Co in the catalyst; that is, there seems to be an ideal Co/Ni ratio that can provide the ideal operation without metal oxidation and carbon formation.

#### 4.2. Nature of the Co–Ni/TiO<sub>2</sub> catalysts for CH<sub>4</sub>/CO<sub>2</sub> reforming

Now the parameters/nature of the catalyst that affect the catalytic activity, stability, and the carbon deposition will be discussed. From TPR spectra for Co–Ni/TiO<sub>2</sub> (Fig. 1), the reduction of metal oxide would be complete below 800 K. The crystallite sizes of the metal before and after the reaction (Table 1) and BET surface areas were similar among all of the catalysts. CO chemisorption capacity is the only parameter that varied for the reduced catalysts, which increased

with increasing Ni content. Hence, the TOF was calculated from the amounts of CO chemisorbed and compared among the catalysts. In fact, 10 mol% nickel substitution in the cobalt catalyst improved the TOF (4.2 s<sup>-1</sup>), and the values remained constant, even when more nickel was added, up to 80 mol%. The excess of nickel in the catalyst (90–100 mol%) led to a higher TOF (4.7–4.9 s<sup>-1</sup>) but also to carbon formation. As can be seen in Fig. 7, there is no proportional relationship between the catalytic activity and the Co/Ni ratio. It is more likely that the metal property was changed by the formation of alloy with a different Co/Ni ratio, to exhibit the synergistic effects of cobalt and nickel in terms of the reactivity for the reforming.

It is generally known that CH<sub>4</sub> can decompose only on the metal surface, not on the support, whereas CO<sub>2</sub> can also be activated on the support [7,8,36]. In the current study, all Co–Ni/TiO<sub>2</sub> catalysts consisted of the same support and same treatment, implying that the support effects should be comparable among the catalysts. Therefore, the reaction with only methane was investigated because it should reflect the metal properties directly. CH<sub>4</sub> pulse reaction results (Table 2) indicate that the CoNi(50:50)/TiO<sub>2</sub> catalyst showed moderate activity between the Ni catalyst and the Co catalyst. The turnover number (TON) of CH<sub>4</sub> converted over the CoNi(50:50)/TiO<sub>2</sub> catalyst was much higher than that over the Co catalyst. It is assumed that the decomposition of methane provides hydrogen to the catalyst (CH<sub>4</sub> → C + 2H<sub>2</sub>). Therefore, it is concluded that the improvement of CH<sub>4</sub> decomposition activity observed for the bimetallic catalyst suppresses the oxidation of metal during the reforming. On the other hand, the Ni/TiO<sub>2</sub> catalyst showed even higher activity for CH<sub>4</sub> than CoNi(50:50)/TiO<sub>2</sub>. Higher activity for CH<sub>4</sub> decomposition leaves a larger amount of coke species on the metal surface, which becomes inactive carbon and therefore has to be removed to proceed with reforming. This control of CH<sub>4</sub> decomposition activity explains why the Co–Ni/TiO<sub>2</sub> catalyst showed higher tolerance to carbon formation than did Ni/TiO<sub>2</sub>. To conclude, the catalyst with the appropriate Co/Ni ratio could inhibit both metal oxidation and carbon formation *kinetically* during CH<sub>4</sub>/CO<sub>2</sub> reforming.

Furthermore, the oxidation of the Co–Ni metal alloy for CoNi(50:50)/TiO<sub>2</sub> took place at a higher temperature than the oxidation of monometallic Co catalyst (see Fig. 6). It is suggested that the Co–Ni alloy on TiO<sub>2</sub> was more resistant to oxidation to the titanate phase than was monometallic cobalt. The formation of alloy enhances the resistance to the unfavorable oxidation of the metal, giving more stable activity for the reforming.

It is possible to control the rate of reactions between oxidative (CO<sub>2</sub>, H<sub>2</sub>O) and the reductive (CH<sub>4</sub>, CO, H<sub>2</sub>) species on the catalyst surface [15,16,30]. Our results suggest that, together with the strong interaction of TiO<sub>2</sub> with metal [16], the metal surface on the catalysts with appropriate activity can be designed by adjustment of the appropriate composite of cobalt and nickel to avoid any deactivation of

the catalyst. The beneficial effects of alloying Ni to Co for CH<sub>4</sub>/CO<sub>2</sub> reforming are (1) promotion of the catalytic reactivity, especially CH<sub>4</sub> activation on the metallic surface, and (2) improvement of the tolerance to the undesirable metal oxidation. The knowledge obtained through this study can be applied further to develop highly efficient catalysts for CH<sub>4</sub>/CO<sub>2</sub> reforming.

## 5. Conclusions

CO<sub>2</sub> reforming of CH<sub>4</sub> was carried out over bimetallic Co–Ni/TiO<sub>2</sub> catalysts with different Co/Ni ratios. The bimetallic Co–Ni/TiO<sub>2</sub> catalysts showed highly stable activities. XRD and XPS analyses revealed that a homogeneous alloy of cobalt and nickel was formed after the H<sub>2</sub> reduction and remained after the reaction. The monometallic Co/TiO<sub>2</sub> catalyst deactivated rapidly because of the oxidation of metal during the reaction. The small nickel substitution of cobalt (10 mol%) dramatically improved the catalytic activity and stability. Compared with the monometallic cobalt catalyst, the bimetallic catalysts improved the resistance to oxidation to form titanate and the reactivity toward CH<sub>4</sub> decomposition on the metal, giving a more reductive atmosphere over the catalyst (e.g., H<sub>2</sub> as a product). With the excess of nickel content (>80 mol%), the catalyst showed higher activity for the CH<sub>4</sub> decomposition and the reforming, but also caused more carbon formation. With appropriate adjustment of the ratio of cobalt and nickel loading, the catalyst provides an optimum balance between the reactions of CH<sub>4</sub> and CO<sub>2</sub>. Long-lived Co–Ni/TiO<sub>2</sub> catalysts that can be used without inducing carbon formation or metal oxidation have been developed for CH<sub>4</sub>/CO<sub>2</sub> reforming.

## Acknowledgments

The authors thank Dr. K. Inazu for his help with the XPS measurements.

## References

- [1] M.C.J. Bradford, M.A. Vannice, *Catal. Rev. Sci. Eng.* 41 (1999) 1, and literatures therein.
- [2] J.R. Rostrup-Nielsen, in: J.R. Anderson, M. Boudart (Eds.), *Catalysis, Science and Technology*, vol. 5, Springer, Berlin, 1984, Chapter 1.
- [3] J.R. Rostrup-Nielsen, *Catal. Today* 37 (1997) 225.
- [4] D.L. Trimm, *Catal. Today* 37 (1997) 233.
- [5] A. Erdöhelyi, J. Cserényi, F. Solymosi, *J. Catal.* 141 (1993) 287.
- [6] Z. Zhang, V.A. Tsipouriari, A.M. Efstathiou, X.E. Verykios, *J. Catal.* 158 (1996) 51.
- [7] M.C.J. Bradford, M.A. Vannice, *Appl. Catal. A* 142 (1996) 73.
- [8] J.H. Bitter, K. Seshan, J.A. Lercher, *J. Catal.* 176 (1998) 93.
- [9] K. Nagaoka, K. Seshan, K. Aika, J.A. Lercher, *J. Catal.* 197 (2001) 34.
- [10] K. Nagaoka, M. Okamura, K. Aika, *Catal. Commun.* 2 (2001) 255.
- [11] M.C.J. Bradford, M.A. Vannice, *Catal. Lett.* 48 (1997) 31.
- [12] T. Osaki, *J. Chem. Soc., Faraday Trans.* 93 (1997) 643.
- [13] K. Nagaoka, K. Takanabe, K. Aika, *Chem. Commun.* (2002) 1006.
- [14] K. Nagaoka, K. Takanabe, K. Aika, *Appl. Catal. A* 255 (2003) 13.
- [15] K. Nagaoka, K. Takanabe, K. Aika, *Appl. Catal. A* 268 (2004) 151.
- [16] K. Takanabe, K. Nagaoka, K. Nariai, K. Aika, *J. Catal.* 230 (2005) 75.
- [17] S.J. Tauster, S.C. Fung, R.T. Garten, *J. Am. Chem. Soc.* 100 (1978) 170.
- [18] S.J. Tauster, S.C. Fung, R.T.K. Baker, J.A. Horsley, *Science* 211 (1981) 1121.
- [19] K. Tomishige, Y. Himeno, Y. Matsuo, Y. Yoshinaga, K. Fujimoto, *Ind. Eng. Chem. Res.* 39 (2000) 1891.
- [20] H.-B. Zhang, P. Chen, G.-D. Lin, K.-R. Tsai, *Appl. Catal. A* 166 (1998) 343.
- [21] M.G. González, N.N. Nichio, B. Moraweck, G. Martin, *Mater. Lett.* 45 (2000) 15.
- [22] J.-S. Choi, K.-I. Moon, Y.G. Kim, J.S. Lee, C.-H. Kim, D.L. Trimm, *Catal. Lett.* 52 (1998) 43.
- [23] S.-H. Seok, S.H. Choi, E.D. Park, S.H. Han, J.S. Lee, *J. Catal.* 209 (2002) 6.
- [24] F. Besenbacher, I. Chorkendorff, B.S. Clausen, B. Hammer, A.M. Molenbroek, J.K. Nørskov, I. Stensgaard, *Science* 279 (1998) 1913.
- [25] H.S. Bengaard, J.K. Nørskov, J. Sehested, B.S. Clausen, L.P. Nielsen, A.M. Molenbroek, J.R. Rostrup-Nielsen, *J. Catal.* 209 (2002) 365.
- [26] C.H. Bartholomew, G.D. Weatherbee, G.A. Jarvi, *Chem. Eng. Commun.* 5 (1980) 125.
- [27] V.R. Choudhary, V.H. Rane, A.M. Rajput, *Appl. Catal. A* 162 (1997) 235.
- [28] V.R. Choudhary, A.M. Rajput, B. Prabhakar, A.S. Mamman, *Fuel* 77 (1998) 1803.
- [29] V.R. Choudhary, A.S. Mamman, *J. Chem. Technol. Biotechnol.* 73 (1998) 345.
- [30] E. Ruckenstein, H.Y. Wang, *J. Catal.* 205 (2002) 289.
- [31] W.C. Conner Jr., G.M. Pajonk, S.J. Teichner, *Adv. Catal.* 34 (1986) 1.
- [32] W.C. Conner Jr., J.L. Falconer, *Chem. Rev.* 95 (1995) 759.
- [33] H.P. Klug, L.E. Alexander, *X-Ray Diffraction Procedures*, Wiley, New York, 1974.
- [34] J.H.A. Martens, H.F.J. van't Blik, R. Prins, *J. Catal.* 97 (1986) 200.
- [35] V. Ponec, *Adv. Catal.* 32 (1983) 149.
- [36] A.N.J. van Keulen, K. Seshan, J.H.B.J. Hoebink, J.R.H. Ross, *J. Catal.* 166 (1997) 306.